Supporting Information for

Synthesis of Supported Ni@(RhNi-alloy) Nanocomposites as an Efficient Catalyst towards Hydrogen Generation from $N_2H_4BH_3$

Changming Li, Yibo Dou, Jie Liu, Yudi Chen, Shan He, Min Wei,* David G. Evans

and Xue Duan

State Key Laboratory of Chemical Resource Engineering, Beijing University of Chemical

Technology, Beijing 100029, P. R. China

[*] Corresponding author. Tel: +86-10-64412131; Fax: +86-10-64425385.

E-mail address: weimin@mail.buct.edu.cn

Experimental section

1. Materials

Rhodium(III) chloride hydrate, sodium borohydride ($NaBH_4$, 99%), and hydrazine hemisulfate (($N_2H_4)_2 \cdot H_2SO_4$) were purchased from Sigma Aldrich. The poly(vinyl pyrrolidone) (PVP, MW=550 000) and ethylene glycol (EG, 99%) were bought from J&KCHEMICA[®]. The following analytical grade inorganic chemicals were used without further purification: $Ni(NO_3)_2 \cdot 6H_2O$, $Al(NO_3)_3 \cdot 9H_2O$, NH_4F. Deionized water was used in all the experimental processes.

2. Synthesis of Ni@(RhNi-alloy)/Al$_2$O$_3$ catalyst

Hierarchical NiAl-LDHs precursor: the hierarchical NiAl-LDHs with molar ratio of $[Ni^{2+}]/[Al^{3+}]=75/25$ were synthesized by a urea decomposition method with the assistance of NH_4F as morphology control agent. In brief, the $Ni(NO_3)_2 \cdot 6H_2O$, $Al(NO_3)_3 \cdot 9H_2O$, urea, and NH_4F were dissolved in 100 mL of deionized water to give a transparent solution with the concentration of 0.075 M, 0.025 M, 0.5 M and 0.2 M, respectively. The resulting solution was aged in a sealed-Teflon autoclave at 383 K for 12 h. The obtained precipitation was washed thoroughly with water and dried in an oven at 60 ºC overnight.

Hierarchical Ni/Al$_2$O$_3$: the hierarchical Ni/Al_2O_3 was obtained *via* an *in situ* reduction process of the NiAl-LDHs precursor. In a typical procedure, 1.0 g of NiAl-LDHs was reduced in a H_2/N_2 (50/50, v/v) stream at 450 °C for 4 h, with an initial heating rate of 2 °C/min. The reduction process results in the phase transformation from LDHs to supported metal catalysts. The resulting product was slowly cooled to the room temperature in a N_2 stream.

Hierarchical Ni@Rh/Al$_2$O$_3$: the Ni@Rh/Al$_2$O$_3$ sample was obtained through the chemical etching of the Ni/Al$_2$O$_3$ sample by RhCl$_3$ aqueous solution following the reaction: $3Ni+2Rh^{3+}=2Rh+3Ni^{2+}$. In a typical process, the RhCl$_3$ aqueous solution is added to the fresh Ni/Al$_2$O$_3$ sample in N$_2$ atmosphere under vigorous stiring. The initial Ni/Rh ratio was fixed to be 16/1. After 5 min, the solution color changes from deep red (RhCl$_3$) to light green (NiCl$_2$), indicating the occurrence of chemical etching reaction. The resulting slurry was washed thoroughly with water and ethanol. The product was dried in a vacuum oven at room temperature.

Hierarchical Ni@(RhNi-alloy)/Al$_2$O$_3$ catalyst: the Ni@(RhNi-alloy)/Al$_2$O$_3$ sample was obtained by calcination of Ni@Rh/Al$_2$O$_3$ in H$_2$ atmosphere at 450 °C for 4 h.

3. Synthesis of hierarchical Ni$_{15}$Rh-alloy/Al$_2$O$_3$ catalysts

Hierarchical NiRhAl-LDHs precursor: the NiRhAl-LDHs with molar ratio of [Ni^{2+}]/[Rh^{3+}]/[Al^{3+}]=75/5/20 was synthesized by a similar method of NiAl-LDHs described above.

Hierarchical Ni$_{15}$Rh-alloy/Al$_2$O$_3$ catalysts: the supported Ni$_{15}$Rh-alloy/Al$_2$O$_3$ catalyst was obtained *via* an *in situ* reduction process of the NiRhAl-LDHs precursor in a H$_2$/N$_2$ (50/50, v/v) stream at 450 °C for 4 h, with an initial heating rate of 2 °C/min.

4. Synthesis of Rh NPs

The Rh NPs were prepared by the colloidal synthesis method according to the previous report.[1] Typically, RhCl$_3$·3H$_2$O and PVP are dissolved in appropriate amount of EG with sonication and aged in a sealed-Teflon autoclave at 403 K for 2 h (RhCl$_3$·3H$_2$O = 0.02 mol·L^{-1}; Rh/PVP = 1/15).

5. Synthesis of hierarchical mixed Rh-Ni/Al$_2$O$_3$ catalyst

The mixed Ni-Rh/Al_2O_3 catalyst was obtained by deposition of Rh NPs on the as-synthetized Ni/Al_2O_3 sample. In a typical process, the Rh NPs colloid was first dispersed in ethanol, and then the Ni/Al_2O_3 sample was added under vigorous stiring for 5 min (Ni/Rh molar ratio was 15/1). Subsequently, acetone was introduced to the suspension as the precipitant of Rh NPs. The resulting product was washed thoroughly with cyclohexane and ethanol, and dried in a vacuum oven at room temperature.

6. Catalysts characterization

Hydrogen temperature programmed reduction (H_2-TPR) was conducted in a quartz tube reactor on a Micromeritics ChemiSorb 2720 with a thermal conductivity detector (TCD). In each case, 100 mg of a sample was sealed in the reactor, and then a gaseous mixture of H_2 and Ar (1:9, v/v) was fed into the reactor at 40 mL/min. The temperature was raised to 1000 °C at a heating rate of 10 °C/min. Powder XRD measurements were performed on a Rigaku XRD-6000 diffractometer, using Cu Kα radiation ($\lambda = 0.15418$ nm) at 40 kV, 40 mA, with a scanning rate of 10°/min, and a 2θ angle ranging from 3° to 90°. The element content in the samples was determined by ICP-AES (Shimadzu ICPS-7500). The morphology of the samples was investigated using a Zeiss Supra 55 scanning electron microscope (SEM) with an accelerating voltage of 20 kV, combined with energy dispersive X-ray spectroscopy (EDS) for the determination of metal composition. Transmission electron microscopy (TEM) images were recorded with JEOL JEM-2010 high resolution transmission electron microscopes. The accelerating voltage was 200 kV. A Tecnai G2 F30 S-TWIN microscope operated at 300 kV was employed to reveal the core–shell stucture using the STEM mode with EDS line or maping scan. The purity of the as-synthetized $N_2H_4BH_3$ was determined by AV600 liquid NMR using CD_3CN as solvent. The product gas was analysed by gas chromatography (GC,

Shimadzu, 2014C) equipped with a thermal conductivity detector (TCD).

7. Catalytic evaluation towards hydrogen generation from $N_2H_4BH_3$ (HB) decomposition

The $N_2H_4BH_3$ (HB) was synthetized according to the previous report.[2] In a typical process, 21.59 g of hydrazine hemisulfate and 10.12 g of sodium borohydride were transferred in a 500 ml three-necked round-bottom flask, followed by addition of 150 ml of dioxane in a argon atmosphere. The mixture was kept under stirring at 30 ºC for 48 h. Subsequently, the filtrate was dried in vacuum overnight to obtain the white solid $N_2H_4BH_3$. The XRD and NMR characterization (Fig. S11) confirm the successful synthesis of HB with the purity of 99.2%. ^1H NMR (δ/ppm, probe head Dual ^1H/^{13}C, CD_3CN, 30 ºC, J/HZ): 5.45 (s, 2H, B-NH$_2$), 3.44 (s, 2H, N-NH$_2$), 1.42(q, 3H, $^1J_{HB}$=95 Hz).

The catalytic activity towards hydrolysis of HB was evaluated by measuring the generation rate of hydrogen along with nitrogen. The scheme of experimental setup is shown in Fig. S12. The catalyst was dispersed in a solution of HB (50 mM, 10 ml), and the total (Ni+Rh)/HB was fixed to be 1/10 for all the catalysts. The generated hydrogen volume was measured *via* a gas volumetric method in an appropriate reaction chamber with thermostatic bath, wherein the temperature was kept constant. The reaction system was sealed and stirred at 800 rpm at 50 ºC.
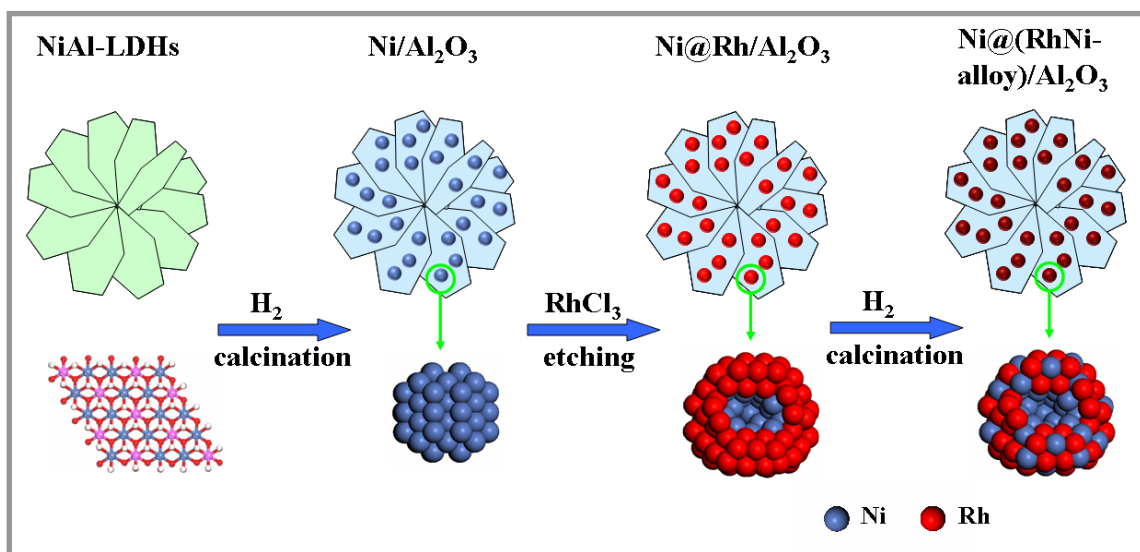
Scheme S1. Schematic representation for the preparation of Ni/Al$_2$O$_3$, Ni@Rh/Al$_2$O$_3$, and Ni@(RhNi-alloy)/Al$_2$O$_3$ *via* a bottom-up method based on LDHs precursor.
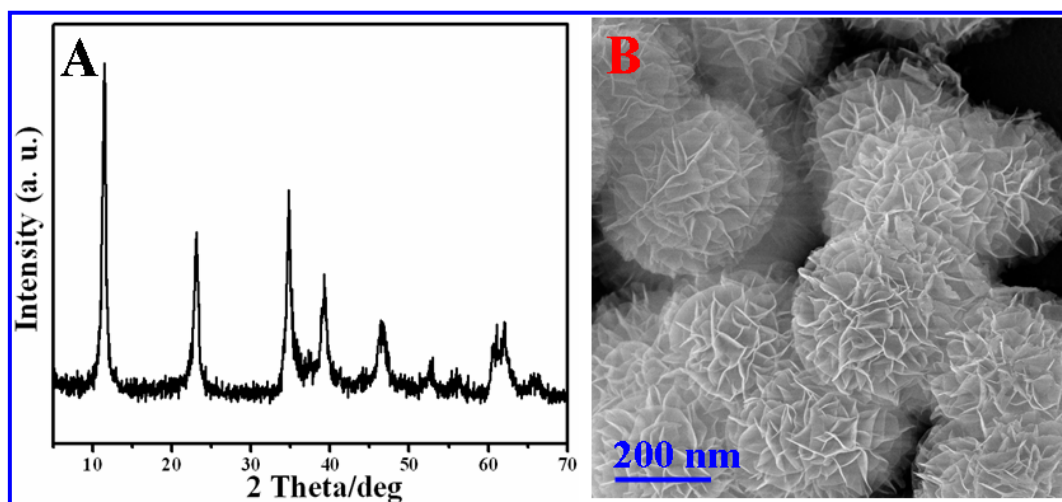

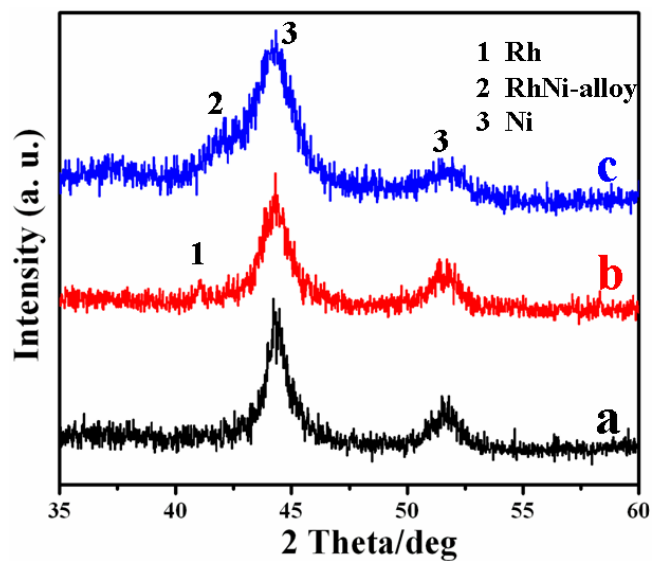**Fig. S1.** (A) XRD pattern and (B) SEM image of the as-synthesized NiAl-LDHs precursor.

Fig. S2. XRD patterns of: (a) Ni/Al$_2$O$_3$ obtained by the reduction of NiAl-LDHs precursor, (b) Ni@Rh/Al$_2$O$_3$, (c) Ni@(RhNi-alloy)/Al$_2$O$_3$.
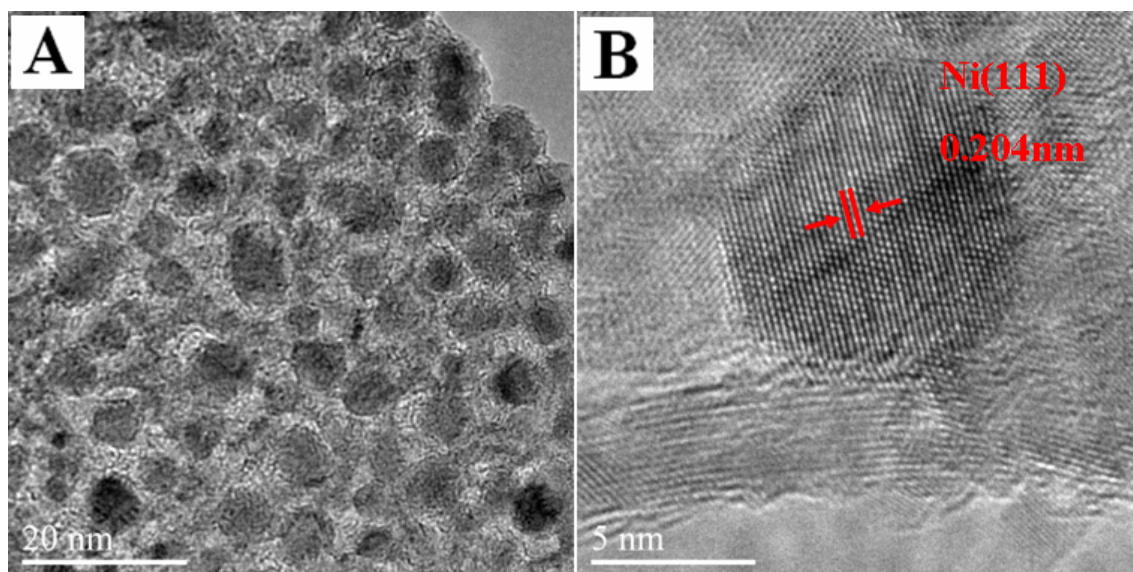

Fig. S3. HRTEM images of Ni/Al$_2$O$_3$ derived from NiAl-LDHs precursor: (A) low magnification image, (B) high magnification image of a single Ni NP.
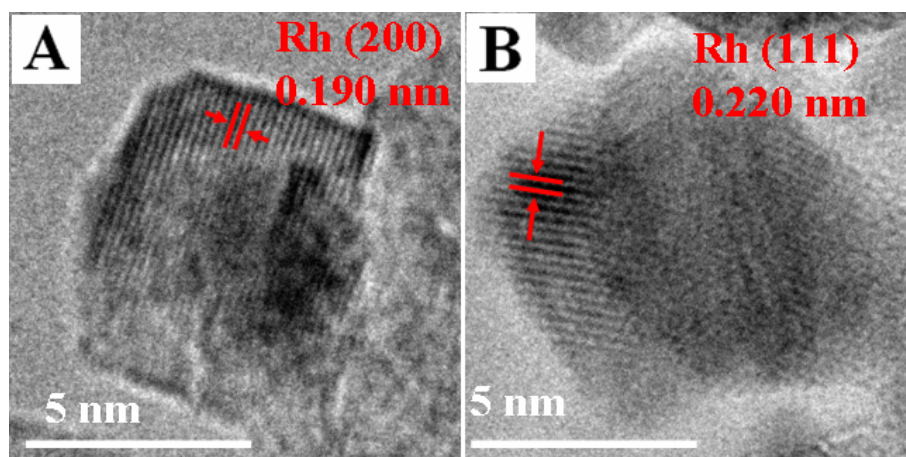
Fig. S4. HRTEM images of a singel Ni@Rh NP obtained by chemical etching of Ni/Al$_2$O$_3$ in RhCl$_3$ aqueous solution.
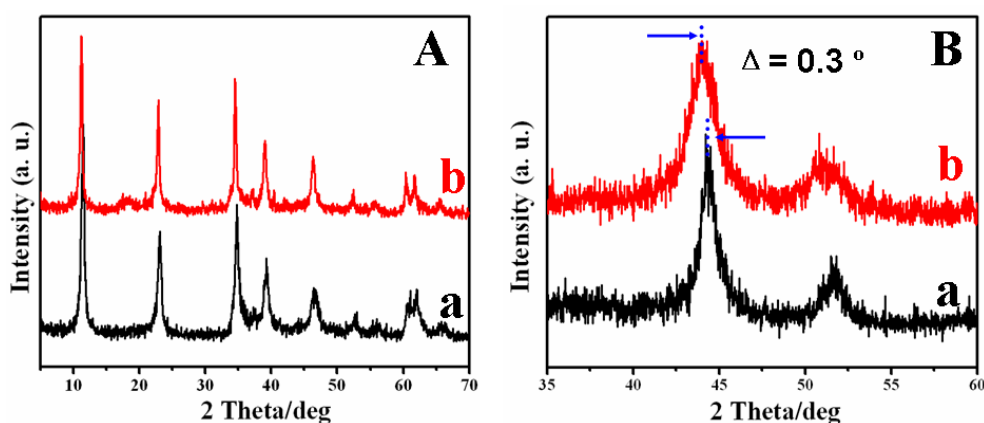

Fig. S5. (A) XRD patterns of the as-synthesized NiAl-LDHs (a) and NiRhAl-LDHs (b); (B) XRD patterns of the Ni/Al$_2$O$_3$ (a) and Ni$_{15}$Rh-alloy/Al$_2$O$_3$ (b).

The identification of Ni$_{15}$Rh-alloy/Al$_2$O$_3$ sample: the Ni$_{15}$Rh-alloy/Al$_2$O$_3$ sample was synthetized by the calcination of ternary NiRhAl-LDH precursor. Compared with the XRD pattern of NiAl-LDHs, a little shift towards low 2θ for NiRhAl-LDHs was observed, indicating the incorporation of Rh element in the LDHs (Fig. S5A). H$_2$-TPR characterization (Fig. S6) reveals a middle reduction temperature of NiRhAl-LDHs (276.5 °C) between NiAl-LDHs (361.2 °C) and

Rh(OH)$_3$/MgAl-LDHs (58.6 ºC), suggesting the formation of Rh-Ni alloy after reduction.[3] The reduction product exhibits XRD reflections at 2θ 43.97 º and 51.02 º, ~0.3 º less than those of pristine Ni phase, confirming the formation of Rh$_{15}$Ni alloy (Fig. S5B). The SEM images with the EDS spectrum (Fig. S7A1−A3) demonstrate the flower-like morphology of both the NiRhAl-LDHs and the reduction product Ni$_{15}$Rh-alloy/Al$_2$O$_3$, in which Rh element is distributed across the hierarchical sphere. The TEM and HRTEM images (Fig. S7B1−B3) reveal the well-dispersed Ni$_{15}$Rh NPs (3−10 nm) on the nanosheet matrix with a lattice distance of 0.207 nm, a little larger relative to pure Ni (0.204 nm).
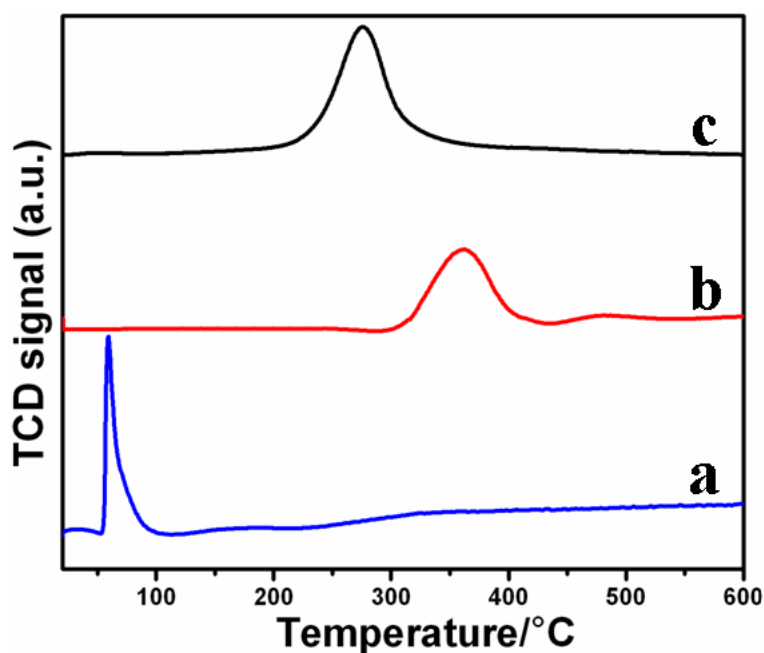

Fig. S6. H$_2$-TPR profiles of (a) Rh(OH)$_3$/MgAl-LDHs, (b) NiAl-LDHs, (c)NiRhAl-LDHs.
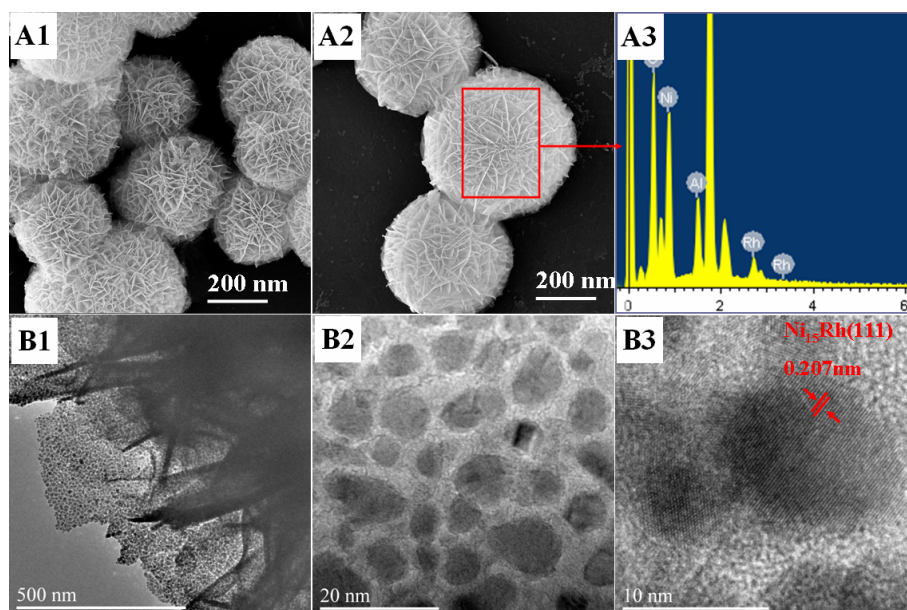
Fig. S7. SEM images of (A1) NiRhAl-LDHs, (A2) $Ni_{15}Rh$-alloy/Al_2O_3 with EDS spectrum (A3); (B1, B2) low and high magnification TEM images of $Ni_{15}Rh$-alloy/Al_2O_3; (B3) HRTEM image of a single $Ni_{15}Rh$ NP.
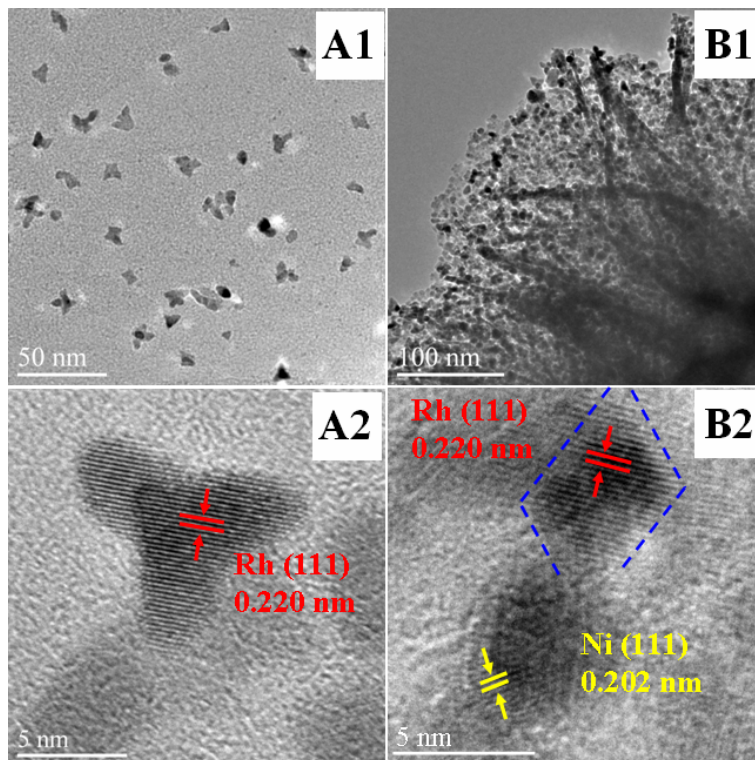

Fig. S8. (A1, A2) TEM and HRTEM images of Rh NPs; (B1, B2) TEM and HRTEM images of the mixed Ni-Rh/Al_2O_3.

The identification of the mixed Rh-Ni/Al$_2$O$_3$ sample: for the as-synthetized Rh NPs, TEM image reveals the multipod-type morphology with 3−5 nm width of branch (Fig. S8-A1). The lattice distance of 0.220 nm can be assigned to Rh (111) interplanar spacing (Fig. S8-A2). The mixed Rh-Ni/Al$_2$O$_3$ sample was obtained by the deposition of Rh NPs on the as-synthetized Ni/Al$_2$O$_3$ sample. The hierarchical morphology can be still maintained as shown in Fig. S8-B1. The HRTEM image further confirms the successful deposition of Rh NPs on the surface of Ni/Al$_2$O$_3$ sample (Fig. S8-B2). In conclusion, based on the LDHs precursor approach, we successfully parpared four different types of supported Ni-Rh nanocomposites (Ni@Rh/Al$_2$O$_3$, Ni@(RhNi-alloy)/Al$_2$O$_3$, Ni$_{15}$Rh-alloy/Al$_2$O$_3$, and mixed Rh-Ni/Al$_2$O$_3$) with similar architectural feature.
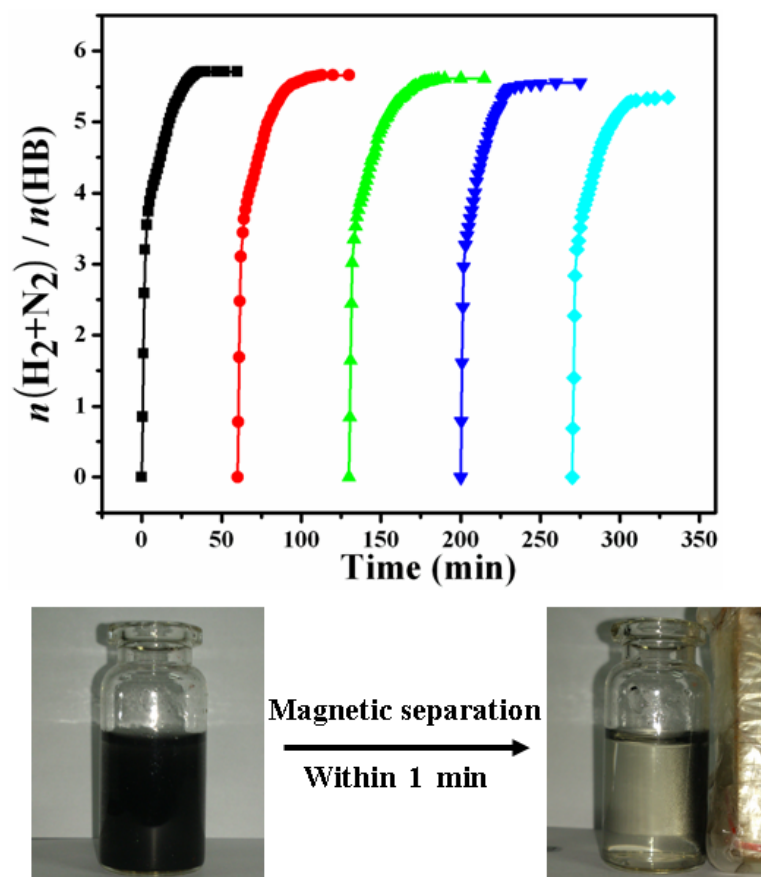
Fig. S9. Hydrogen generation from N$_2$H$_4$BH$_3$ over Ni@(RhNi-alloy)/Al$_2$O$_3$ catalyst for 5 consecutive cycles by magnetic separation ([HB] = 50 mM, (Rh+Ni)/HB=0.1, T = 50 °C).
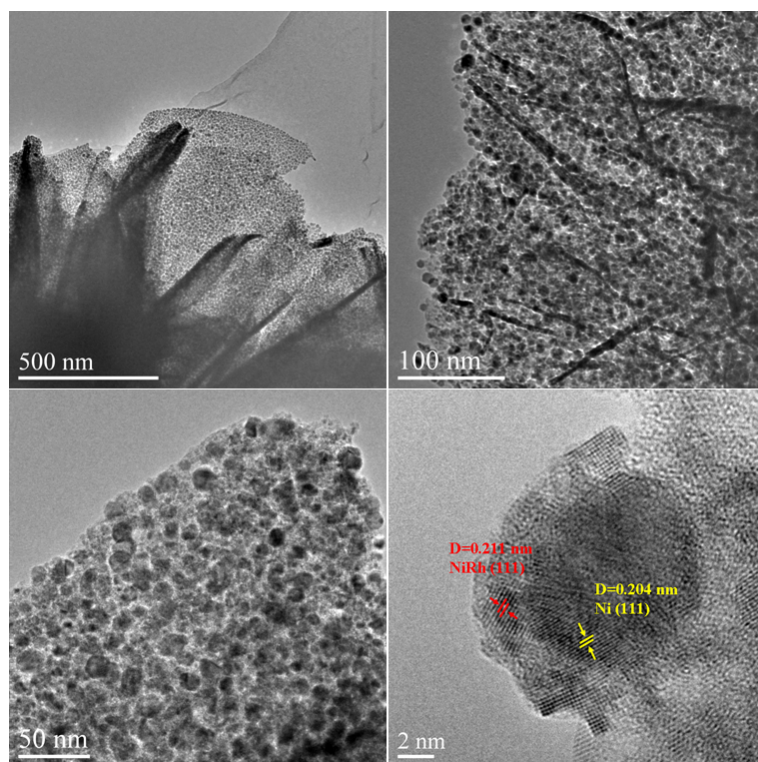
Fig. S10. TEM images of the used Ni@(RhNi-alloy)/Al$_2$O$_3$ catalyst after 5 catalytic recycles at different scales.
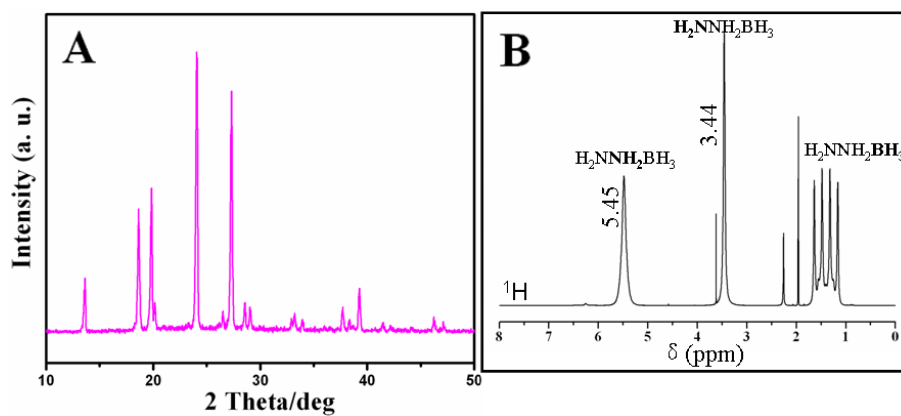

Fig. S11. The XRD pattern and ^{1}H NMR spectrum of the as-obtained N$_2$H$_4$BH$_3$.
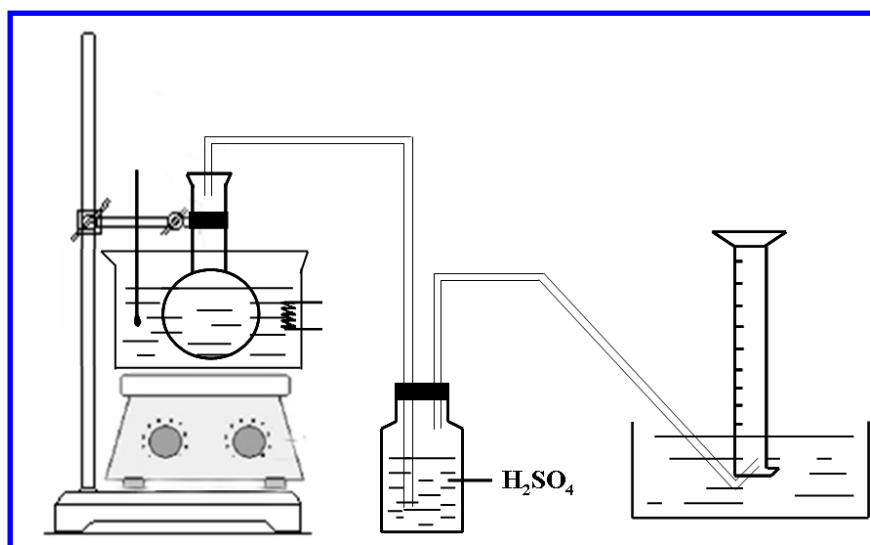
Fig. S12. The experimental setup for hydrogen generation from $N_2H_4BH_3$ dehydrogenation.

References:

1 H. Asakura, K. Teramura, T. Shishido, T. Tanaka, N. Yan, C. X. Xiao, S. Y. Yao and Y. Kou, *Phys. Chem. Chem. Phys.*, 2012, **14**, 2983. (Rh)

2 R. Moury, G. Moussa, U. B. Demirci, J. Hannauer, S. Bernard, E. Petit, A. V. D. Lee and P. Miele, *Phys. Chem. Chem. Phys.*, 2012, **14**, 1768.

3 L. He, Y. Q. Huang, A. Wang, Y. Liu, X. Y. Liu, X. W. Chen, J. J. Delgado, X. D. Wang and T. Zhang, *J. Catal.*, 2013, **298**, 1.